Received: 27 September 2022 | Revised: 31 January 2023 | Accepted: 5 February 2023

DOI: 10.1002/ags3.12665

AGSurg Annals of Gastroenterological Surgery Open Access WILEY

ORIGINAL ARTICLE

Circ_0102543 suppresses hepatocellular carcinoma progression through the miR-942-5p/SGTB axis

Shiming Yang[1] | Dianye Wang[2] | Rui Zhang[3]

[1]Department of General Surgery, Shanxi Provincial People's Hospital, Taiyuan, China

[2]Department of Cardiovascular, Affiliated Hospital of Shanxi University of Traditional Chinese Medicine, Taiyuan, China

[3]Department of Hepatobiliary and Pancreatic Surgery, Liver Transplantation Center, The First Hospital of Shanxi Medical University, Taiyuan, China

Correspondence
Shiming Yang. MM Department of General Surgery, Shanxi Provincial People's Hospital, No. 29 Shuangtasi street, Taiyuan 030000, Shanxi, China.
Email: ysm561@126.com

Abstract

Introduction: Hepatocellular carcinoma (HCC) is one of the most serious cancers. Circular RNA (circRNA) has been reported to regulate the progression of HCC. Herein, the role of circ_0102543 in HCC tumorigenesis was investigated.

Materials: The expression levels of circ_0102543, microRNA-942-5p (miR-942-5p), and small glutamine rich tetratricopeptide repeat co-chaperone beta (SGTB) were detected by quantitative real-time PCR (qRT-PCR). 3-(4, 5-dimethylthiazol-2-yl)-2,5-diphenyltetrazolium Bromide (MTT) assay, thymidine analog 5-ethynyl-2'-deoxyuridine (EDU) assay, transwell assay, and flow cytometry were conducted to explore the function of circ_0102543 in HCC cells and the regulatory mechanism among circ_0102543, miR-942-5p and SGTB in HCC cells. Western blot examined the related protein levels.

Results: The expression of circ_0102543 and SGTB was decreased in HCC tissues, while the expression of miR-942-5p was increased. Circ_0102543 acted as a sponge for miR-942-5p, and SGTB was the target of miR-942-5p. Circ_0102543 upregulation hindered tumor growth in vivo. In vitro experiments showed that overexpression of circ_0102543 significantly repressed the malignant behaviors of HCC cells, while co-transfection of miR-942-5p partially attenuated these effects mediated by circ_0102543. In addition, SGTB knockdown increased the proliferation, migration, and invasion of HCC cells inhibited by miR-942-5p inhibitor. Mechanically, circ_0102543 regulated SGTB expression in HCC cells by sponging miR-942-5p.

Conclusion: Overexpression of circ_0102543 suppressed proliferation, migration, and invasion of HCC cells by regulating the miR-942-5p/SGTB axis, suggesting that circ_0102543/miR-942-5p/SGTB axis may be a potential therapeutic target for HCC.

KEYWORDS
circ_0102543, hepatocellular carcinoma, miR-942-5p, SGTB

1 | INTRODUCTION

Hepatocellular carcinoma (HCC) is the most common primary liver cancer, ranking the fourth highest mortality rate among all cancers[1,2]. Although there has been some progress in the treatment of liver cancer, the metastasis and recurrence rates of liver cancer patients is high, leading to low survival rate and poor prognosis[3]. Therefore, it is necessary to study the pathogenesis of HCC and explore new therapeutic targets.

Circular RNAs (CircRNAs) are one of the non-coding RNAs formed by covalently linking the 3' and 5' ends, which can regulate cancer

progression[4,5]. Similarly, circRNAs have been reported to regulate HCC progression. For example, Ding et al. showed the up-regulation of circ_0001955 in HCC by microarray analysis, which could promote the proliferation of HCC cells[6]. CircRNAs have been found to act as competing endogenous RNAs (ceRNAs) that can regulate the expression of target mRNAs through sponging microRNAs (miRNA)[7,8]. Zang et al. showed that circ_0000517 might contribute to HCC progression by regulating miR-1296-5p[9]. Previous studies have shown that double PHD fingers 3 (DPF3) was significantly down-regulated in breast cancer, and silencing of DPF3 could promote the proliferation of breast cancer cells[10]. Besides, DPF3 is one of the cancer predisposition genes, and might contribute to the regulation of the HCC pathway by increasing survival, altering oncogenic expression and affecting DNA damage[11]. Circ_0102543 is a new identified circRNA that is produced by the back-splicing of DPF3 genes on the chr14: 73181130–73198642. However, the role of circ_0102543 in HCC has not been studied.

MiRNAs are small non-coding RNAs consisting of about ~22 nucleotides[12,13]. Recently, the regulatory role of miR-942-5p in the carcinogenesis has been reported. For example, up-regulated miR-942-5p repressed the proliferation of colorectal cancer[14]. Moreover, miR-942-5p was significantly increased in HCC cells, and its elevation facilitated the proliferation of HCC cells[15]. In addition, we found that small glutamine rich tetratricopeptide repeat co-chaperone beta (SGTB) was the target of miR-942-5p, and SGTB has been found to be correlated with cancer progression, among which, it has been reported that SGTB could promote the malignant behaviors of HCC cells[16]. However, whether miR-942-5p or SGTB is regulated by circ_0102543 in HCC has not been understood.

Here, we showed that circ_0102543 had the ability to affect HCC cell proliferation, metastasis, and apoptosis. Moreover, we identified a novel circ_0102543/miR-942-5p/SGTB ceRNA network in HCC progression.

2 | METHODS

2.1 | Human subject study

In this study, we obtained 61 pairs of HCC tumors and adjacent normal tissues (ANT, at least 2 cm away from the neoplastic mass) from HCC patients who underwent surgical resection at Shanxi Provincial People's Hospital. All tissues were confirmed to be HCC by postoperative pathological examination. None of the patients received any preoperative treatment. Human tissue samples were stored in the refrigerator at −80°C for subsequent experiments. The study protocol was approved by the Ethics Committee of Shanxi Provincial People's Hospital and research subjects gave informed consent.

2.2 | Cell lines and cell transfection

Human liver immutable cell lines (THLE-2) and human HCC cells lines (Huh-7, MHCC97H, MHCC97L and SNU449) were purchased from American Type Culture Collection (ATCC; Manassas, VA, USA). All cells were cultured in DMEM medium (Thermo Fisher, Waltham, MA, USA) containing 10% FBS and 1% double antibodies and placed in a cell incubator with 5% CO_2 at 37°C.

To overexpress circ_0102543, the full-length cDNA of circ_0102543 was amplified and then cloned into over expression vector pLO5-ciR (RiboBio, Guangzhou, China), which contained a front and back circular frame, while the mock vector with no circ_0102543 sequence served as a control (vector)[17]. The miR-942-5p mimic (miR-942-5p) and its control group (miR-NC), miR-942-5p inhibitor (in-miR-942-5p) and its control group (in-miR-NC), and the SGTB-specific siRNA (si-SGTB) and si-NC were also synthesized by RiboBio (Guangzhou, China). Then 100 ng circ_0102543, 50 nM miR-942-5p mimic or inhibitor, 100 ng si-circ_0102543 or the same account of controls were transfected into Huh-7 and MHCC97H cells using Lipofectamine 2000 (Thermo Fisher).

2.3 | Quantitative real-time polymerase chain reaction (qRT-PCR)

Isolation of total RNA was conducted using TRIzol reagent (Takara, Beijing, China), and then reverse transcribed into cDNA using random hexamers with PrimeScript RT Reagent Kit (Takara). The All-in-One miRNA First stand cDNA Synthesis Kit (GeneCopoeia, Rockville, MD, USA) were used to synthesize cDNA from miRNA. Thereafter, qRT-PCR analysis was performed using TB Green Premix Ex Taq (Takara) on a Bio-Rad CFX96 system (Bio-Rad, CA, USA). GAPDH or U6 was used as the internal reference, and the relative expression was calculated by $2^{-\Delta\Delta CT}$ method. A list of primer sequences was available in Table S1.

2.4 | RNase R treatment

Total RNA (3 μg) was incubated with or without 3 U/μg of RNase R (Epicenter Technologies, Madison, WI, USA) at 37 °C for 1 h, then qRT-PCR was conducted to determine the expression levels of circ_0102543 and DPF3 mRNA.

2.5 | Western blot analysis

The total protein of each group was extracted using RIPA lysis buffer (Solarbio, Beijing, China), and determined by a BCA kit (Pierce; Rockford, IL, USA). About 30 μg proteins were subjected to SDS-PAGE electrophoresis. After electrophoresis, the protein on the gel was transferred to the PVDF membrane (Millipore, Billerica, MA, USA) by wet transfer, and the primary antibodies againstβ-actin (1:1000, ab8226, Abcam, Cambridge, MA, USA), cyclin D1 (1:200, ab16663, Abcam), Epithelial cadherin (E-cadherin; 1:1000, ab231303, Abcam), Neuronal cadherin (N-cadherin;

1:1000, ab76011, Abcam), cleaved caspase-3 (cleaved casp-3; 1:1000, ab2302, Abcam), and SGTB (1:1000, ab202419, Abcam) were used to incubate with the membrane overnight. Then the membrane was incubated with HRP-conjugated secondary antibodies for 1 h. Lastly, protein bands were assessed by using Clarity™ Western ECL Substrate Kit (Bio-Rad, Shanghai, China) and ECL system (Pierce). In each independent experiment, three parallel wells were made, and the procedures were carried out in triplicate.

2.6 | Cell proliferation assay

After transfection, Huh-7 and MHCC97H cells were added into 96-well plates at a density of 1×10^4 cells/well. For 3-(4, 5-dimethylthiazol-2-yl)-2, 5-diphenyltetrazolium bromide (MTT) assay, when the cells were incubated in 96-well plates for 24, 48, 72, or 96 h, 10 μL MTT reagent (Sigma, St Louis, MO, USA) was added into each well, followed by 100 μL DMSO to dissolve formazan. Finally, the absorbance at 570 nm was detected by a microplate reader (Bio-Rad, Hercules, CA, USA).

For thymidine analog 5-ethynyl-2'-deoxyuridine (EdU) assay, EdU incorporation assay kit (RiboBio) was applied to detect the positive cells. Huh-7 and MHCC97H cells were added to 96-well plate containing EdU medium diluent and cultured for 2 h in line with the instruction. Following being fixed and permeabilized, cell nuclei were counterstained with DAPI. Finally, photographs were taken, and stained cells were analyzed under a fluorescence microscope (Nikon, Tokyo, Japan).

2.7 | Transwell assay

For cell migration analysis, cell medium was changed to serum-free medium before the experiment, and the cells were starved overnight. A 200 μL serum-free cell suspension was inoculated in the upper chamber of transwell insert, and 600 μL DMEM medium containing 10% FBS was added into the lower chamber for 24 h culture. After washing with PBS solution, cells on the upper chamber were gently wiped using the cotton ball, cells on the lower chamber were fixed with formaldehyde for 30 min, and then stained with 0.1% crystal violet solution for 30 min. The number of migrated cells were observed under a microscope (Bio-Rad). For cell invasion analysis, the upper layer of transwell was coated with Matrigel, and the other steps were the same as described above.

2.8 | Flow cytometry assay

Transfected Huh-7 and MHCC97H cells were resuspended in 200 μL binding buffer (containing 10 μL Annexin-FITC) and incubated for 30 min. Then 5 μL Propidium iodide (PI, BD Biosciences, San Diego, CA, USA) and 300 μL binding buffer were added. Apoptosis rate was analyzed by flow cytometry.

2.9 | Dual-luciferase reporter assay

The fragments of circ_0102543 and SGTB 3'UTR containing the binding site of miR-942-5p were amplified by qRT-PCR, then circ_0102543-WT and SGTB 3'UTR-WT vectors were constructed, and circ_0102543-MUT and SGTB 3'UTR-MUT vectors were constructed by point mutation kit (Beyotime, Shanghai, China). These vectors were co-transfected into Huh-7 and MHCC97H cells with miR-942-5p mimic or miR-NC. The luciferase activity of cells was detected by dual-luciferase activity detection kit (GeneCopoeia, Rockville, MD, USA).

2.10 | RNA immunoprecipitation (RIP) assay

RIP assay was performed using an Imprint RNA immunoprecipitation kit (Sigma). Transfected or non-transfected Huh-7 and MHCC97H cells were lysed in RIP lysis buffer. Cell lysate was incubated with magnetic beads coupled with human anti-Argonaute2 (anti-Ago2) or negative control anti-IgG for 12 h at 4°C. The relative enrichments of miR-942-5p and circ_0102543 were measured by qRT-PCR.

2.11 | Immunohistochemistry (IHC)

The anti-Ki-67 (1:2,00, ab15580; Abcam) and anti-SGTB (1:1000, ab202419, Abcam), biotinylated goat anti-rabbit IgG secondary antibody (1:300, ab64256, Abcam) and 3,3-diaminobenzidine (DAB) kits (Vector Laboratories, Peterborough, UK) were used for IHC analysis based on standard methods[18].

2.12 | Xenograft models

All animal experiments were carried out in accordance with the instructions of Shanxi Provincial People's Hospital Animal Care and Use Committee. BALB/C mice (6–8 weeks of age) were provided by Beijing Weida River Laboratory Animal Science and Technology Co., LTD (Beijing, China). All mice were fed with standard diet and were housed in a temperature-controlled room with a 12-h dark/light cycle for 1 week prior to the experiments. Huh-7 cells (5×10^6) transfected with lentivirus carrying vector or circ_0102543 were subcutaneously injected into BALB/C mice ($n = 5$/group). The length and width of the tumor were measured weekly, and the volume was calculated according to the formula (volume = length×width^2/2). After 4 weeks, the mice were euthanized by cervical dislocation under 2% isoflurane anesthesia and the tumors were removed and weighed. The expression of circ_0102543 and miR-942-5p in tumors were analyzed by qRT-PCR.

2.13 | Statistical analysis

All experiments were repeated three times, the final data were expressed as mean ± standard deviation (SD). In case of multiple comparison, Bonferroni correction was applied. The differences between two groups were compared by Student's *t*-test, and, if not normally distributed, by Mann–Whitney test. The differences of more than two groups were evaluated using the ANOVA followed by post hoc testing. The correlation between two variables was analyzed by Pearson analysis. All analyses were conducted by GraphPad Prism 7 software, and $P < 0.05$ indicates significant difference.

3 | RESULTS

3.1 | Circ_0102543 was down-regulated in HCC tissue and cells

Circ_0102543 is a new identified circRNA that is produced by the back-splicing of DPF3 genes on the chr14: 73181130-73198642, and the result of Sanger sequencing confirmed the head-to-tail splicing in the qRT-PCR product of circ_0102543 (Figure 1A). Furthermore, we discovered that compared with DPF3 mRNA, circ_0102543 was resistant to RNase R digestion, implying that circ_0102543 was a circRNA (Figure S3). In total, 61 HCC patients were enrolled in this study and the expression of circ_0102543 was found to be substantially down-regulated in cancer tissues (Figure 1B). We further analyzed the correlation between circ_0102543 expression and clinicopathological parameters of HCC patients, the results showed that low expression level of circ_0102543 was significantly correlated with the advance TNM stage, lymph node metastasis, and fibrosis (Table 1). Then patients were divided into two groups based on the median level of circ_0102543, the overall survival rate of the high circ_0102543 expression group was significantly higher than that of the group with low circ_0102543 expression (Figure 1C). Moreover, compared with normal THLE-2 cells, circ_0102543 expression was also significantly decreased in the HCC cell lines, especially in Huh-7 and MHCC97H cells (Figure 1D). Therefore, Huh-7 and MHCC97H cells were selected for subsequent functional experiments. These data indicated the down-regulation of circ_0102543 in HCC tissues and cells.

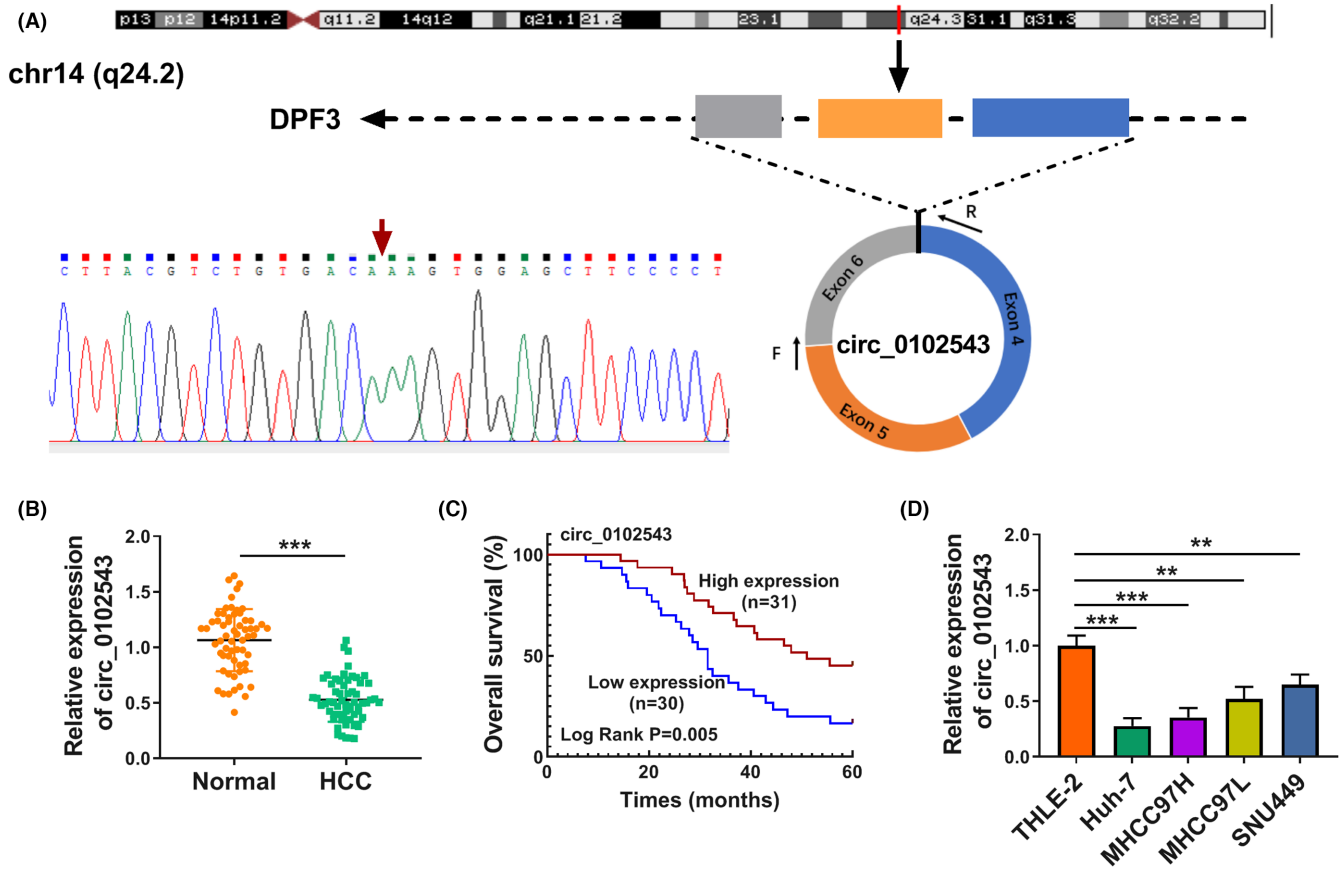

FIGURE 1 Circ_0102543 was downregulated in HCC tissues and cell lines. (A) A scheme illustrating the formation of circ_0102543, and the specific primers of circ_0102543 were validated by Sanger sequencing. (B) The expression of circ_0102543 in HCC tissues and normal tissues ($n = 61$) was tested by qRT-PCR (Student's *t*-test). (C) Kaplan–Meier percent survival curves were used to evaluate the overall survival of HCC patients with high or low circ_0102543 expression. (D) qRT-PCR detected the expression of circ_0102543 in HCC cells (one-way ANOVA). $^{**}P < 0.01$, $^{***}P < 0.001$.

TABLE 1 Correlation between circ_0102543 expression and clinicopathological features in HCC patients ($N = 61$).

Characteristic	circ_0102543		*P*-value
	High ($N = 31$)	Low ($N = 30$)	
Age (year)			0.7972
<60	19	17	
≥60	12	13	
Gender			0.2016
Male	11	16	
Female	20	14	
Tumor size			0.0409
<5 cm	10	18	
≥5 cm	21	12	
TNM stage			0.0214
I-II	10	19	
III-IV	21	11	
HBsAg			0.7863
Positive	22	20	
Negative	9	10	

Abbreviation: HBsAg: Hepatitis B surface antigen.

3.2 | Overexpression of circ_0102543 inhibited the malignant behaviors of HCC cells

Gene manipulation of circ_0102543 was performed using overexpression vector, qRT-PCR verified the transfection efficiency of circ_0102543 (Figure 2A,B). MTT assay showed that circ_0102543 significantly reduced the proliferation of Huh-7 and MHCC97H (Figure 2C,D). EdU positive Huh-7 and MHCC97H cells were consistently lower in circ_0102543 overexpression group than that of the control group (Figure 2E), further suggesting that overexpression of circ_0102543 depressed HCC cell proliferation. The migration and invasion of Huh-7 and MHCC97H cells transfected with circ_0102543 were significantly reduced (Figure 2F,G). However, flow cytometry showed that circ_0102543 overexpression significantly promoted apoptosis (Figure 2H). Molecularly, western blot showed that circ_0102543 overexpression significantly reduced the expression of CyclinD1 and N-cadherin, and increased E-cadherin levels and the ratio of Cleaved-casp3/pro-casp3 (Figure 2I,J). Taken together, these data suggested that overexpression of circ_0102543 suppressed HCC cell malignant behaviors.

3.3 | Circ_0102543 interacted with miR-942-5p

In order to further explore the downstream targets of circ_0102543, circinteractome (https://circinteractome.nia.nih.gov/mirna_target_sites.html) database was applied. And the binding sites of circ_0102543 and miR-942-5p predicted by circinteractome were showed in Figure 3A. Dual-luciferase reporter assay results showed that the combined transfection of miR-942-5p and circ_0102543-WT in Hun-7 and MHCC97H cells significantly inhibited the luciferase activity, while co-transfection of miR-942-5p and circ_0102543-MUT showed no significant change in the luciferase activity (Figure 3B,C). The RIP assay showed that circ_0102543 and miR-942-5p were enriched in Ago group compared with the normal IgG group (Figure 3D,E), and were highly enriched in cells transfected with miR-942-5p mimics compared with the controls (Figure S2A,B). By using starbase database, we compared the expression of miR-942-5p in HCC and normal tissues. The mean level of miR-942-5p was higher in HCC tissues than those in normal tissues (Figure S1). Subsequently, we detected the expression of miR-942-5p in HCC tissues and cells by qRT-PCR, and the results also showed that the expression of miR-942-5p in HCC tissues and cells was significantly increased (Figure 3F,G). Moreover, miR-942-5p level was notably decreased in HCC cells by the overexpression of cricDPF3 (Figure 3H,I). Therefore, the above data show that miR-942-5p was the target of circ_0102543.

3.4 | Overexpression of miR-942-5p alleviated the inhibitory effects of circ_0102543 on HCC cell malignant behaviors

As shown in Figure 4A, miR-942-5p level was increased in Huh-7 and MHCC97H cells transfected with miR-942-5p. Functionally, the MTT and EDU assays showed that co-transfection of miR-942-5p restored the cell proliferation down-regulated by circ_0102543 (Figures 4B–D). Meanwhile, the transwell assay showed that the addition of miR-942-5p restored the migration and invasion rates of Huh-7 and MHCC97H cells decreased by circ_0102543 (Figure 4E,F). Mechanically, flow cytometry showed that circ_0102543 increased the apoptosis rate of Huh-7 and MHCC97H cells, which was decreased by miR-942-5p (Figure 4G). Similarly, western blot results showed that co-transfection of miR-942-5p up-regulated the CyclinD1 and N-cadherin proteins that were down-regulated by circ_0102543, and miR-942-5p down-regulated the E-cadherin level and Cleaved-casp3/pro-casp3 ratio increased by circ_0102543 (Figure 4H,I). These data suggested that circ_0102543 might regulate the proliferation, migration, and invasion of HCC cells by targeting miR-942-5p.

3.5 | MiR-942-5p targeted SGTB

We predicted that SGTB was the target of miR-942-5p using the bioinformatics tool StarBase 3.0 (http://starbase.sysu.edu.cn/agoClipRNA.php?source=mRNA). And the binding sites of miR-942-5p and SGTB are shown in Figure 5A. Dual-luciferase reporter assay results showed that the co-transfection of miR-942-5p and SGTB 3'UTR-WT significantly inhibited luciferase activity, while the co-transfection of miR-942-5p and SGTB

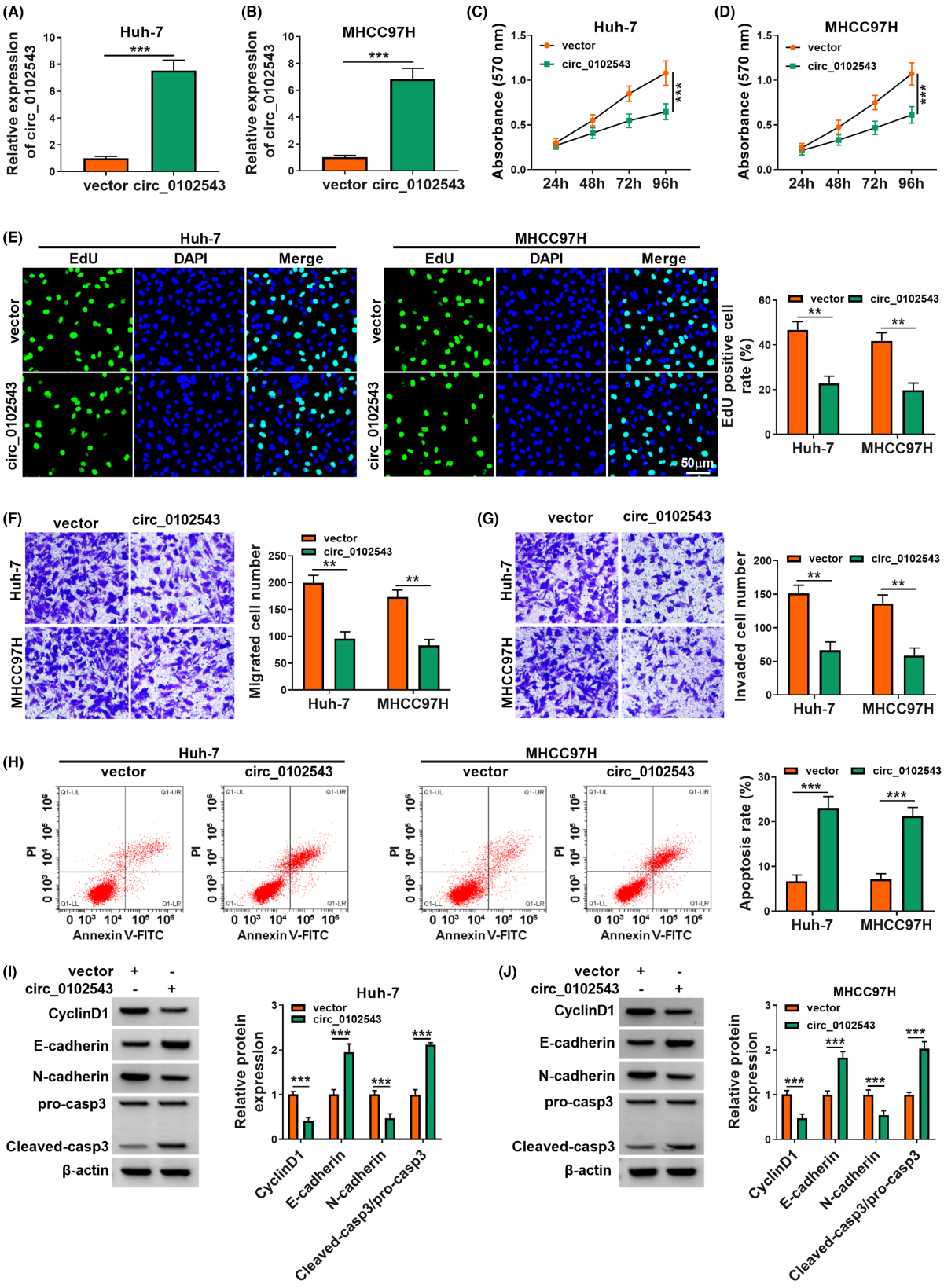

FIGURE 2 The functional roles of circ_0102543 in HCC cells. (A, B) The expression of circ_0102543 was determined by qRT-PCR assay in Huh-7 and MHCC97H cells transfected with vector or circ_0102543 (Student's *t*-test). (C, D) MTT was used to detect cell proliferation (two-way ANOVA). (E) EDU proliferation assay was performed in transfected Huh-7 and MHCC97H cells (two-way ANOVA). (F, G) Cell migration and invasion were monitored by transwell assay (two-way ANOVA). (H) Flow cytometry was used to detect cell apoptosis (two-way ANOVA). (I) The expression level of CyclinD1, E-cadherin, N-cadherin, Cleaved-casp3, and pro-casp3 was determined by western blot (two-way ANOVA). $^{**}P<0.01$, $^{***}P<0.001$.

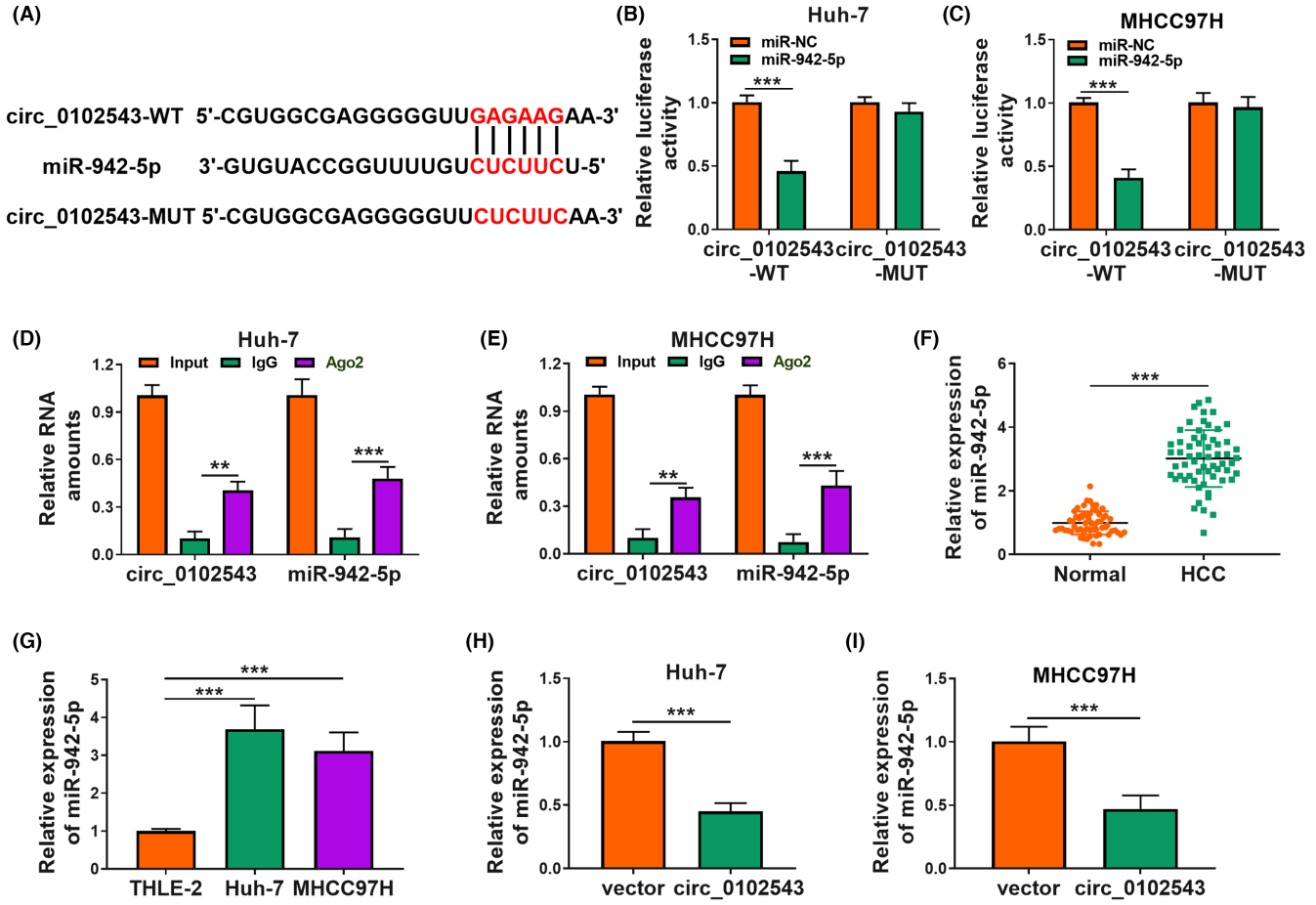

FIGURE 3 Circ_0102543 functioned as a sponge of miR-942-5p. (A) The complementary sequences between miR-942-5p and circ_0102543 were showed. (B, C) Dual-luciferase reporter assay was performed to confirm the association between miR-942-5p and circ_0102543 (two-way ANOVA). (D, E) The relationship between miR-942-5p and circ_0102543 was verified by RIP assay (two-way ANOVA). (F) The expression of miR-942-5p in HCC tissues and normal tissues ($n = 61$) was tested by qRT-PCR (Student's t-test). (G) Levels of miR-942-5p in HCC cell lines and normal cell lines were detected by qRT-PCR (one-way ANOVA) (H, I) The expression of miR-942-5p detected by qRT-PCR (Student's t-test). $^{**}P < 0.01$, $^{***}P < 0.001$.

3'UTR-MUT showed no significant change in luciferase activity (Figure 5B,C). Subsequently, we detected the expression of SGTB in HCC tissues by qRT-PCR, and the results showed that the expression of SGTB in HCC tissues was significantly decreased (Figure 5D). And IHC assay also showed the significant reduction of SGTB in HCC tissues (Figure 5E). Similarly, SGTB was lowly expressed in Huh-7 and MHCC97H cells (Figure 5F). Mechanically, western blot showed that SGTB was remarkably suppressed by miR-942-5p overexpression (Figure 5G). Then, qRT-PCR validated the transfection efficiency of in-miR-942-5p (Figure 5H). And the level of SGTB was found to be increased by in-miR-942-5p (Figure 5I). Lastly, western blot results showed that circ_0102543 transfection significantly increased the expression of SGTB, while co-transfection with miR-942-5p downregulated its expression (Figure 5J,K). Additionally, there were a negative correlation between miR-942-5p and circ_0102543 or SGTB mRNA expression, and a positive correlation between circ_0102543 and SGTB mRNA expression in HCC tissues (Figure 5L–N). Therefore, the above data show that SGTB was the target of miR-942-5p, and circ_0102543/miR-942-5p/SGTB formed an axis.

3.6 | SGTB silencing alleviated miR-942-5p inhibitor-mediated inhibition of HCC cell malignant behaviors

Western blot showed that si-SGTB could significantly downregulate the expression of SGTB (Figures 6A). Functionally, the si-SGTB eliminated the inhibitory effect of miR-942-5p inhibitor on Huh-7 and MHCC97H cell proliferation (Figure 6B–D). In the same way, the transwell assay showed that the addition of si-SGTB restored the decrease of cell migration and invasion caused by in-miR-942-5p (Figure 6E–H). Mechanically, flow cytometry showed that miR-942-5p inhibitor increased the apoptosis rate of Huh-7 and MHCC97H cells, while si-SGTB decreased

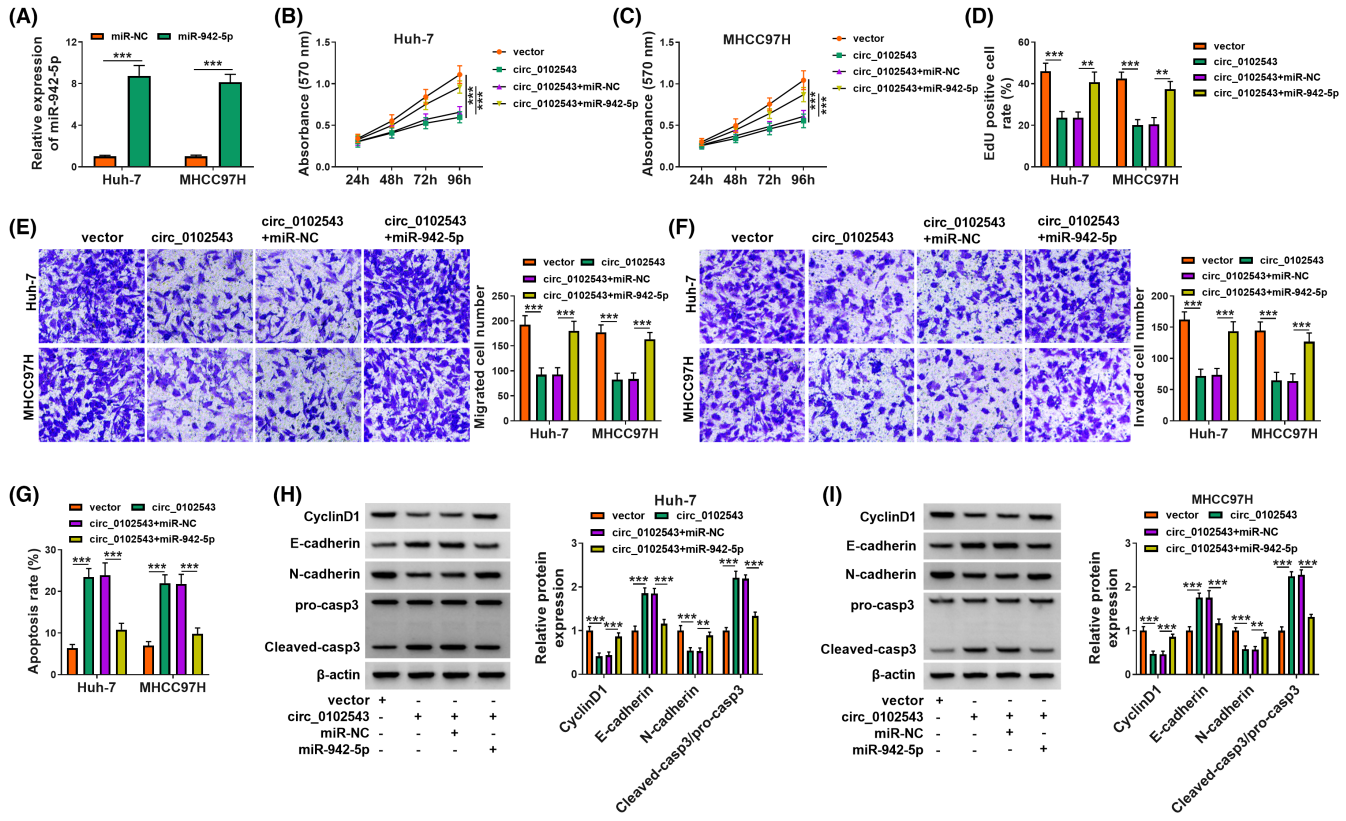

FIGURE 4 Circ_0102543 regulated the proliferation, migration, and invasion by targeting miR-942-5p in HCC cells. (A) The expression level of miR-942-5p was determined by qRT-PCR (two-way ANOVA). (B, C) MTT was used to detect cell proliferation (two-way ANOVA). (D) EDU proliferation assay was performed in transfected Huh-7 and MHCC97H cells (two-way ANOVA). (E, F) Cell migration and invasion were monitored by transwell assay (two-way ANOVA). (G) Flow cytometry was used to detect cell apoptosis (two-way ANOVA). (H, I) The expression level of CyclinD1, E-cadherin, N-cadherin, Cleaved-casp3, and pro-casp3 was determined by western blot (two-way ANOVA). $^{**}P<0.01$, $^{***}P<0.001$.

this effect (Figure 6I). Similarly, western blot results showed that co-transfection of si-SGTB up-regulated the expression of CyclinD1 and N-cadherin proteins and down-regulated the E-cadherin level and Cleaved-casp3/pro-casp3 ratio in miR-942-5p decreased cells (Figure 6J,K). These data suggested that miR-942-5p might regulate the malignant behaviors of HCC cells by targeting SGTB.

3.7 | Overexpression of circ_0102543 restricted the tumorigenicity of HCC cells in vivo

Tumor formation in nude mice was established by Huh-7 cells transfected with circ_0102543 and vector. Overexpression of circ_0102543 significantly reduced the tumor volume and weight (Figure 7A,B). Molecularly, tumors in circ_0102543 group exhibited an upregulation of circ_0102543 level, and downregulation of miR-942-5p level (Figure 7C,D). Furthermore, IHC results showed that the expression of SGTB was significantly increased in the circ_0102543 group, and Ki67 was down-regulated by the overexpression of circ_0102543 (Figure 7E).

4 | DISCUSSION

CircRNA, as a ceRNA, is associated with a variety of human diseases including cancer through sharing miRNAs[19]. Here, we for the first time showed that circ_0102543 acted as a novel regulator of HCC cell functional properties through regulating the miR-942-5p/SGTB axis.

In recent years, more and more researchers have become devoted to exploring the role of circRNAs, a newly discovered endogenous non-coding RNA, in cancers[20,21]. CircRNAs have been proved to play oncogenic or tumor-suppressing genes in the tumorigenesis of breast cancer[22]. ovarian cancer[23]. esophageal cancer[24]. and HCC. For example, circ_0091579 was highly expressed in HCC tissues, and silencing of circ_0091579 blocked the proliferation and metastasis of HCC cells[25]. In addition, a recent finding showed that circ-SMARCA5 was downregulated in HCC, and circ-SMARCA5 overexpression suppressed cell malignant behaviors in HCC[26]. Consistent with these findings, our results confirmed that circ_0102543 was abnormally down-regulated in HCC tissues and cell lines. Nevertheless, low sample size is still our shortcoming, and a larger cohort of sample size will be collected to verify the expression profile and

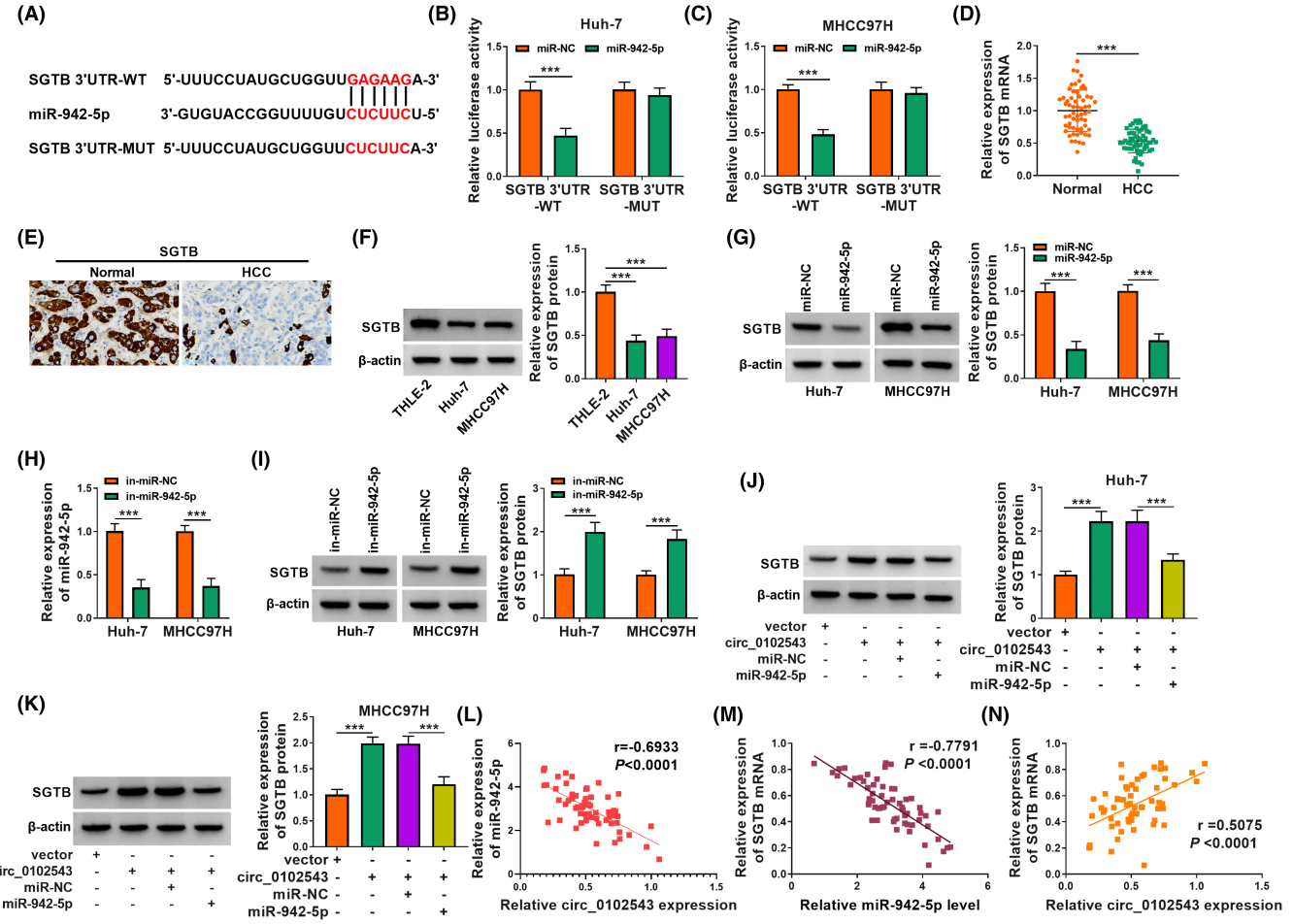

FIGURE 5 SGTB was the direct target of miR-942-5p. (A) The complementary sequences between miR-942-5p and SGTB were showed. (B, C) Dual-luciferase reporter assay was performed to confirm the association between miR-942-5p and SGTB 3'UTR (two-way ANOVA). (D) qRT-PCR detected the expression of SGTB in CC tissues and normal tissues ($n = 61$) (Student's t-test). (E) IHC assay examined the protein level of SGTB in CC tissues and normal tissues ($n = 61$). (F) Western blot assay examined the protein level of SGTB in HCC cells (one-way ANOVA). (G) Western blot was used to detect the protein level of SGTB after miR-942-5p mimic transfection (two-way ANOVA). (H) qRT-PCR detected the expression of miR-942-5p after in-miR-NC or in-miR-942-5p transfection (two-way ANOVA). (I) Western blot detected the expression of SGTB after in-miR-NC or in-miR-942-5p transfection (two-way ANOVA). (J–K) Western blot was used to detect the effects of circ_0102543/miR-942-5p axis on SGTB expression (one-way ANOVA). (L–N) The correlation between miR-942-5p and circ_0102543 or SGTB expression in HCC samples was analyzed by Pearson analysis. ***$P < 0.001$.

clinical role of circ_0102543 in HCC. Functionally, re-expression of circ_0102543 inhibited HCC cell proliferation, migration, and invasion, and promoted cell apoptosis in vitro. In addition, circ_0102543 also inhibited tumor growth in nude mice, indicating that circ_0102543 might play an anticancer role in HCC progression. The entire process of gene overexpression by plasmids is termed a mechanism of RNA overexpression, and adenoviral or lentiviral vectors are often utilized for circRNA overexpression in vivo[27]. In addition to overexpress circRNA by plasmids, direct synthesis and purification of circRNAs can be also employed to produce highly purified circRNA molecules[28]. Importantly, circRNA overexpression-based strategy has limitations that can be typically mitigated using nanoparticle and exosome delivery systems[29]. Therefore, we speculate that circ_0102543-based therapeutics using nanoparticle or exosome may have clinical roles in HCC prevention.

CircInteractome database predicted that circ_0102543 had binding sites with miR-942-5p, and miR-942-5p has been extensively identified as an oncogene. Circ0106714 absorbed miR-942-5p to inhibit the occurrence of colorectal cancer[30]. Similarly, studies have shown that miR-942-5p acted as a promotor in ovarian cancer progression and negatively regulated the inhibitory effects of circ_0015756 on ovarian cancer tumorigenesis[31]. This conclusion was consistent with our research. First, we verified that miR-942-5p expression was notably enhanced in HCC. Subsequently, functional analysis demonstrated that miR-942-5p restored circ_0102543 overexpression-induced inhibition of HCC cell malignant behaviors. It was confirmed that circ_0102543 could regulate HCC cell tumorigenesis via targeting miR-942-5p.

The miRNA can regulate gene expression via binding to the 3'UTR of the target mRNA[32]. It was previously reported that SGTB was a downstream target of miR-1277-5p[33]. At the same

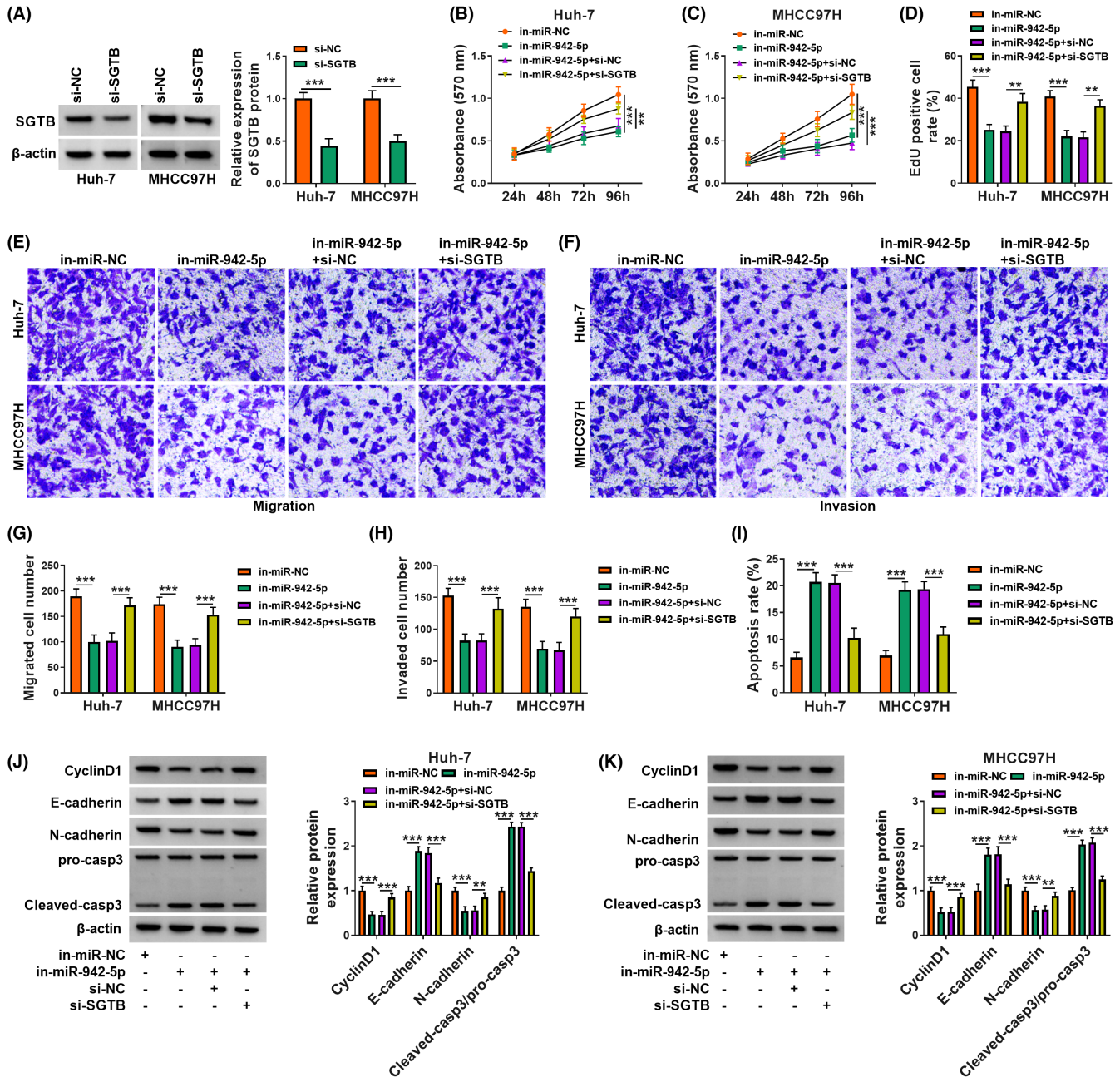

FIGURE 6 MiR-942-5p regulated the proliferation, migration, and invasion by targeting SGTB in HCC cells. (A) The protein level of SGTB was determined by Western blot (two-way ANOVA). (B, C) MTT was used to detect cell proliferation (two-way ANOVA). (D) EDU proliferation assay was performed in transfected Huh-7 and MHCC97H cells (two-way ANOVA). (E–H) Cell migration and invasion were monitored by transwell assay (two-way ANOVA). (I) Flow cytometry was used to detect cell apoptosis (two-way ANOVA). (J, K) The expression level of CyclinD1, E-cadherin, N-cadherin, pro-casp3, and Cleaved-casp3 was determined by western blot (two-way ANOVA). $^{**}P<0.01$, $^{***}P<0.001$.

time, we also proved that SGTB was a target of miR-942-5p. Tian et al. reported that upregulation of miR-365b inhibited the function of SGTB on HCC[16]. Our study made clear that SGTB was diminished in HCC. Functionally, si-SGTB eliminated the suppressing function of miR-942-5p inhibitor on HCC cell malignant behaviors. Mechanically, SGTB expression was elevated by circ_0102543 and subsequently reduced by the addition of miR-942-5p, further implying the mechanism of circ_0102543/miR-942-5p/SGTB in HCC cells. Clinically, circ_0102543 plasmids may synergistically play an anticancer role with miR-942-5p antagonist and/or SGTB plasmids.

In summary, we found that circ_0102543 positively regulated SGTB through sponging miR-942-5p, thereby inhibiting HCC progression. These findings provided new targets for follow-up research and treatment development of HCC.

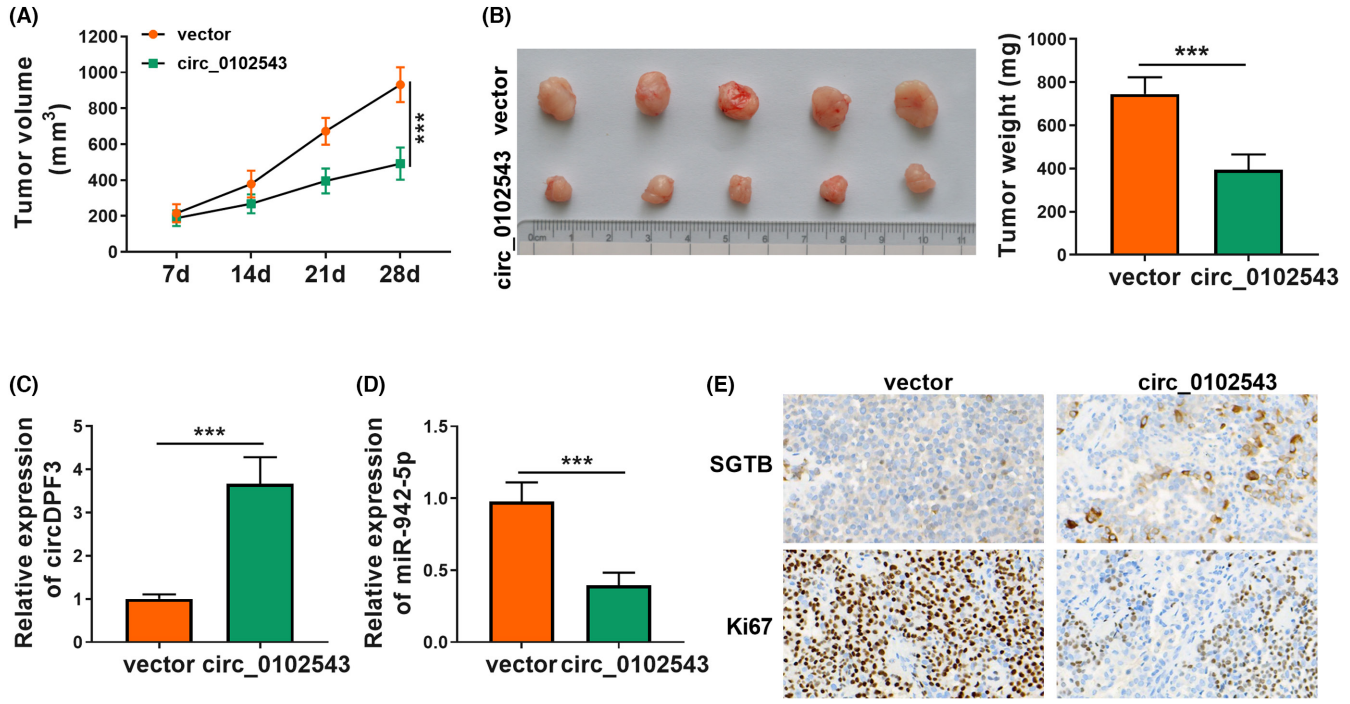

FIGURE 7 Circ_0102543 overexpression inhibited tumor growth in vivo. (A, B) Tumor volume (two-way ANOVA) and weight (Student's *t*-test) after circ_0102543 overexpression in vivo. (C, D) Relative expression levels of circ_0102543 and miR-942-5p in xenografts were detected by qRT-PCR (Student's *t*-test). (G) The positive rates of SGTB and Ki67 were analyzed by IHC. $^*P < 0.05$.

AUTHORS CONTRIBUTIONS

Conceptualization and Methodology: Rui Zhang and Dianye Wang; Formal analysis and Data curation: Shiming Yang and RuiZhang; Validation and Investigation: Shiming Yang and Rui Zhang; Writing—original draft preparation and Writing—review and editing: Shiming Yang, Rui Zhang and Dianye Wang; Approval of final manuscript: all authors.

FUNDING INFORMATION

No funding was received.

CONFLICT OF INTEREST STATEMENT

The authors declare that they have no competing interests.

DATA AVAILABILITY STATEMENT

The datasets used and/or analyzed during the current study are available within the manuscript and its supplementary information files.

ETHICS STATEMENTS

Approval of the research protocol: N/A.

Informed Consent: The present study was approved by the ethical review committee of Shanxi Provincial People's Hospital with approval No. 20210418. Written informed consent was obtained from all enrolled patients.

Registry and the Registration No. of the study/trial: N/A.

Animal Studies: N/A.

Consent for publication: Patients agree to participate in this work.

ORCID

Shiming Yang https://orcid.org/0000-0001-7421-8166

REFERENCES

1. Farazi PA, DePinho RA. Hepatocellular carcinoma pathogenesis: from genes to environment. Nat Rev Cancer. 2006;6(9):674–87.
2. Dutta R, Mahato RI. Recent advances in hepatocellular carcinoma therapy. Pharmacol Ther. 2017;173:106–17.
3. Singh S, Singh PP, Roberts LR, Sanchez W. Chemopreventive strategies in hepatocellular carcinoma. Nat Rev Gastroenterol Hepatol. 2014;11(1):45–54.
4. Memczak S, Jens M, Elefsinioti A, Torti F, Krueger J, Rybak A, et al. Circular RNAs are a large class of animal RNAs with regulatory potency. Nature. 2013;495(7441):333–8.
5. Liu J, Liu T, Wang X, He A. Circles reshaping the RNA world: from waste to treasure. Mol Cancer. 2017;16(1):58.
6. Ding B, Fan W, Lou W. hsa_circ_0001955 enhances In vitro proliferation, migration, and invasion of HCC cells through miR-145-5p/NRAS Axis. Mol Ther Nucleic Acids. 2020;22:445–55.
7. Hansen TB, Kjems J, Damgaard CK. Circular RNA and miR-7 in cancer. Cancer Res. 2013;73(18):5609–12.
8. Hansen TB, Jensen TI, Clausen BH, Bramsen JB, Finsen B, Damgaard CK, et al. Natural RNA circles function as efficient microRNA sponges. Nature. 2013;495(7441):384–8.
9. Zang H, Li Y, Zhang X, Huang G. Circ_0000517 contributes to hepatocellular carcinoma progression by upregulating TXNDC5 via sponging miR-1296-5p. Cancer Manag Res. 2020;12:3457–68.
10. Lin WH, Dai WG, Xu XD, Yu QH, Zhang B, Li J, et al. Downregulation of DPF3 promotes the proliferation and motility of breast cancer cells through activating JAK2/STAT3 signaling. Biochem Biophys Res Commun. 2019;514(3):639–44.
11. Ramos-Lopez O, Riezu-Boj JI, Milagro FI, Alfredo Martinez J. Association of Methylation Signatures at hepatocellular carcinoma

pathway genes with adiposity and insulin resistance phenotypes. Nutr Cancer. 2019;71(5):840–51.
12. Krol J, Loedige I, Filipowicz W. The widespread regulation of microRNA biogenesis, function and decay. Nat Rev Genet. 2010;11(9):597–610.
13. Melo SA, Esteller M. Disruption of microRNA nuclear transport in human cancer. Semin Cancer Biol. 2014;27:46–51.
14. Zhou L, Chen Q, Wu J, Yang J, Yin H, Tian J, et al. miR-942-5p inhibits proliferation, metastasis, and epithelial-mesenchymal transition in colorectal cancer by targeting CCBE1. Biomed Res Int. 2021;2021:9951405.
15. Wang Q, Wu J, Huang H, Jiang Y, Huang Y, Fang H, et al. lncRNA LIFR-AS1 suppresses invasion and metastasis of non-small cell lung cancer via the miR-942-5p/ZNF471 axis. Cancer Cell Int. 2020;20:180.
16. Tian Q, Sun HF, Wang WJ, Li Q, Ding J, Di W. miRNA-365b promotes hepatocellular carcinoma cell migration and invasion by downregulating SGTB. Future Oncol. 2019;15(17):2019–28.
17. Liu F, Zhang X, Wu F, Peng H. Hsa_circ_0088212-mediated miR-520 h/APOA1 axis inhibits osteosarcoma progression. Transl Oncol. 2021;14(12):101219.
18. Zhang S, Cheng J, Quan C, Wen H, Feng Z, Hu Q, et al. circCELSR1 (hsa_circ_0063809) contributes to paclitaxel resistance of ovarian cancer cells by regulating FOXR2 expression via miR-1252. Mol Ther Nucleic Acids. 2020;19:718–30.
19. Karreth FA, Pandolfi PP. ceRNA cross-talk in cancer: when ce-bling rivalries go awry. Cancer Discov. 2013;3(10):1113–21.
20. Zhang HD, Jiang LH, Sun DW, Hou JC, Ji ZL. CircRNA: a novel type of biomarker for cancer. Breast Cancer. 2018;25(1):1–7.
21. Sand M, Bechara FG, Gambichler T, Sand D, Bromba M, Hahn SA, et al. Circular RNA expression in cutaneous squamous cell carcinoma. J Dermatol Sci. 2016;83(3):210–8.
22. Lin G, Wang S, Zhang X, Wang D. Circular RNA circPLK1 promotes breast cancer cell proliferation, migration and invasion by regulating miR-4500/IGF1 axis. Cancer Cell Int. 2020;20(1):593.
23. Hou W, Zhang Y. Circ_0025033 promotes the progression of ovarian cancer by activating the expression of LSM4 via targeting miR-184. Pathol Res Pract. 2020;217:153275.
24. Chen L, Kong R, Wu C, Wang S, Liu Z, Liu S, et al. Circ-MALAT1 functions as both an mRNA translation brake and a microRNA sponge to promote self-renewal of hepatocellular cancer stem cells. Adv Sci. 2020;7(4):1900949.
25. Niu WY, Chen L, Zhang P, Zang H, Zhu B, Shao WB. Circ_0091579 promotes proliferative ability and metastasis of liver cancer cells by regulating microRNA-490-3p. Eur Rev Med Pharmacol Sci. 2019;23(23):10264–73.
26. Yu J, Xu QG, Wang ZG, Yang Y, Zhang L, Ma JZ, et al. Circular RNA cSMARCA5 inhibits growth and metastasis in hepatocellular carcinoma. J Hepatol. 2018;68(6):1214–27.
27. Meganck RM, Borchardt EK, Castellanos Rivera RM, Scalabrino ML, Wilusz JE, Marzluff WF, et al. Tissue-dependent expression and translation of circular RNAs with recombinant AAV vectors In vivo. Mol Ther Nucleic Acids. 2018;13:89–98.
28. Chen YG, Chen R, Ahmad S, Verma R, Kasturi SP, Amaya L, et al. N6-Methyladenosine modification controls circular RNA immunity. Mol Cell. 2019;76(1):96–109.e109.
29. He AT, Liu J, Li F, Yang BB. Targeting circular RNAs as a therapeutic approach: current strategies and challenges. Signal Transduct Target Ther. 2021;6(1):185.
30. Li S, Yan G, Liu W, Li C, Wang X. Circ0106714 inhibits tumorigenesis of colorectal cancer by sponging miR-942-5p and releasing DLG2 via hippo-YAP signaling. Mol Carcinog. 2020;59(12):1323–42.
31. Du Z, Wang L, Xia Y. Circ_0015756 promotes the progression of ovarian cancer by regulating miR-942-5p/CUL4B pathway. Cancer Cell Int. 2020;20(1):572.
32. Lai EC. Micro RNAs are complementary to 3'UTR sequence motifs that mediate negative post-transcriptional regulation. Nat Genet. 2002;30(4):363–4.
33. Wang B, Sun Y, Liu N, Liu H. LncRNA HOTAIR modulates chondrocyte apoptosis and inflammation in osteoarthritis via regulating miR-1277-5p/SGTB axis. Wound Repair Regen. 2021;29(3):495–504.

SUPPORTING INFORMATION

Additional supporting information can be found online in the Supporting Information section at the end of this article.

How to cite this article: Yang S, Wang D, Zhang R. Circ_0102543 suppresses hepatocellular carcinoma progression through the miR-942-5p/SGTB axis. Ann Gastroenterol Surg. 2023;7:666–677. https://doi.org/10.1002/ags3.12665